UCLA - ENG - 8640
October 1986

THERMAL COMPONENTS FOR 1.8 K SPACE CRYOGENICS

By

W. E. W. Chen
W. A. Hepler
T.H. K.Frederking, P.I.

Prepared for the

NATIONAL AERONAUTICS AND SPACE ADMINISTRATION
AMES RESEARCH CENTER
MOFFETT FIELD, CA 94035

Grant NAG 2-412
Summer 1986

School of Engineering and Applied Science
Chem. Eng. Dept.
University of California, Los Angeles
CA 90024

UCLA - ENG - 8640
October 1986

THERMAL COMPONENTS FOR 1.8 K SPACE CRYOGENICS

By

W. E. W. Chen
W. A. Hepler
T.H. K.Frederking, P.I.

Prepared for the

NATIONAL AERONAUTICS AND SPACE ADMINISTRATION
AMES RESEARCH CENTER
MOFFETT FIELD, CA 94035

Grant NAG 2-412
Summer 1986

School of Engineering and Applied Science
Chem. Eng. Dept.
University of California, Los Angeles
CA 90024

TABLE OF CONTENTS

II, III, IV

THERMAL COMPONENTS OF 1.8 K SPACE CRYOGENICS

ABSTRACT

Work of the Summer 1986 is summarized in three areas: first, conceptual design of a laboratory system for heat exchanger evaluation in conjunction with the operation of a thermally activated fountain effect pump (FEP); second, Knudsen effect evaluation of fine porous media useful for the pressurization plug which forms the main component of the FEP; third, proof-of-principle test of the lab system selected on the basis of the evaluation, item (1).

1. INTRODUCTION

The present report presents results of research on thermal components around 1.8 K during the Summer 1986 (NASA Grant NAG 2-412). Motivation for the studies originated with activities centering around applications of the fountain effect in He II, in particular in space cryogenics projects. It is noted though that applied superconductivity has triggered similar activities aiming at the use of coolant circulation in NbTi-based magnets operating at high fields near 1.8 K.

Another space cryogenics area of inquiry has been in the past concerned with vapor-liquid phase separators for He II space vessels. The thermomechanical effect (fountain effect) in this case is used to keep liquid inside the tank, i.e., the thermomechanical force is directed toward the interior of the tank. The porous plugs employed in phase separation mostly have been one order of magnitude away from pump plug data as far as the pore size and characteristic length (L_c = square root of the Darcy permeability) is concerned. Therefore, several transport parameters of the extended flow range have to be known. In addition, the details of heat transport and heat transfer within the fine porous plug of a fountain effect pump (FEP), or close to it are not known to the extent desirable in quantification efforts. The present work has aimed at bringing a simple lab pump system to the proof-of-principle stage. The initial efforts have been directed toward conceptual options available for a small lab dewar geometry (Section 2). Further, Knudsen effects on the transport of gases at room temperature are discussed (Section 3). Results of this nature are useful for a preliminary screening of porous plugs prior to low temperature use. Finally, the proof-of-principle

runs are described (Section 4). Appendix Sections provide additional details about the present work. Appendix A presents simple similarity conditions for the zero net mass flow mode and for finite mass flow in the thermomechanical pump. Appendix B contains details of extended transfer pump tests using the liquid transfer pump developed for phase separator work. Appendix C adds details of the Knudsen effect measurements. Appendix D presents an assessment of the flow conditions of the present proof-of-principle runs.

2. FEP SYSTEM CONCEPTS FOR A SMALL LAB DEWAR TEST FACILITY

The preceding work on vapor liquid phase separation has been conducted with a setup incorporating a long inner tube, serving as vent line, surrounded by a liquid bath. In fact, a dual bath was incorporated to minimize perturbation effects. The porous plug serving as phase separator has been placed at the bottom of the vent tube. Loss of liquid in the "tank" was compensated for by means of liquid transfer from the outer reservoir of the dual vessel system. For this purpose, a small fountain effect pump (FEP) was used. The performance of this pump was re-inspected in the context of the present (Summer 1986) work.

Aside from this experience with a small lab pump, it was desirable to pinpoint the extent of allowable parameters in the efforts toward a viable liquid transfer pump for use of space. The task in this area may be illustrated by reference to a fully instrumented and controlled flow system with upstream and downstream pumps and sensors. An example is Reference 1 of the Klipping group. This type of system would reach a cost bracket probably beyond the order of magnitude of 10^5 dollars (in present dollar value). Therefore, skilled design and application of existing items has been necessary

to come up with a simple solution compatible with the net value of about $12,000 allocated for the Summer 1986 work.

The following design options are outlined: first, a system concept which resembles closely a space system, as visualized for instance by the various groups reporting in the 1985 Space Cryogenics Workshop in Boulder (Guest editor: P. Kittel Ref. 2). Second, a suitable lab flow-through system; third, a simple transfer pump system (Ref. 3).

The first case is illustrated in Figure 1 which outlines a "mini-dual vessel" assembly fitting into the laboratory dewar. The particular lab dewar geometry, favored traditionally, is a long vertical system with rather small diameter and rather large length. This geometry has the disadvantage that vessel-to-vessel transfer is not readily incorporated unless very minute vessel sizes are chosen, as sketched in Fig. 1. These appear to be miniaturization tasks, and a minute transfer line with a small FEP plug has to be compatible with the layout.

The second system is a flow-through assembly which fits into the existing dewar readily. FEP plug and energizing heater have been separated, as shown in the various versions of Figure 2. A relatively tall vacuum can has been envisioned for the system studies. In figure 2a both FEP and heater unit (HE) are lined up horizontally. In Fig. 2b both the FEP and the system HE are in one leg of a U-tube assembly. This has the disadvantage that FEP and heater are rather far apart causing possibly additional losses in energy. Figure 2c presents a version with the FEP at the bottom of the "U" while the heater unit is in one vertical leg. Again there is a certain separation of the FEP from the HE. In Fig. 2d, the FEP and the heater are located in the

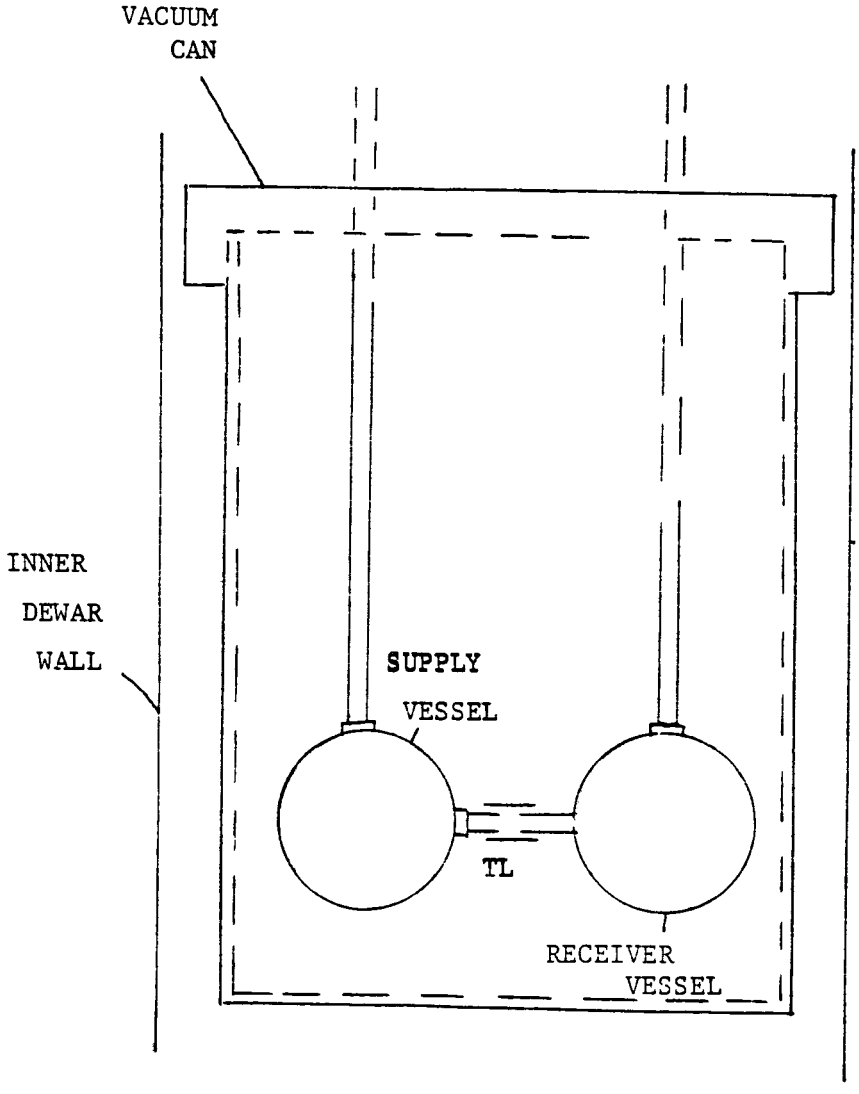

Figure 1. "Mini-Vessel Assembly" in small la_b dewar, schematically;
Existing dewar I.D. approx. 7.5 cm (3 in.)
TL Transfer line with FEP and coupling.

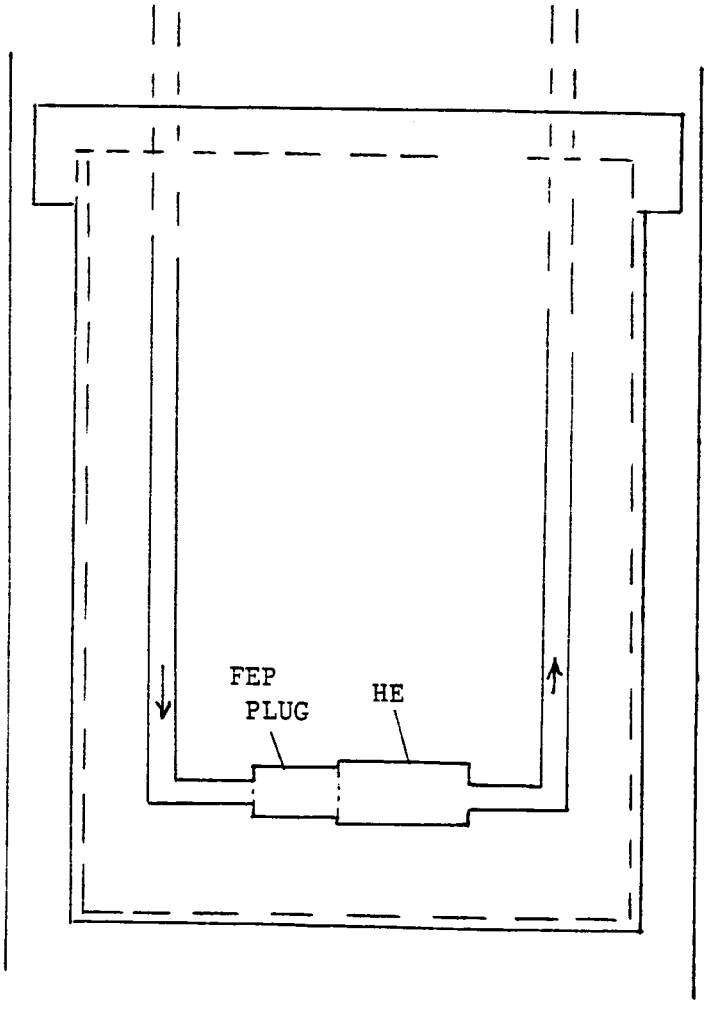

Figure 2 . "FL OW THROUGH" System, schematically
a. Fountain effect pump (FEP) and Heater Unit (HE) arranged horizontally ;
The subsequent figures 2b to 2d illustrate other configurations.

Vacuum can arrangement as in Fig.1.

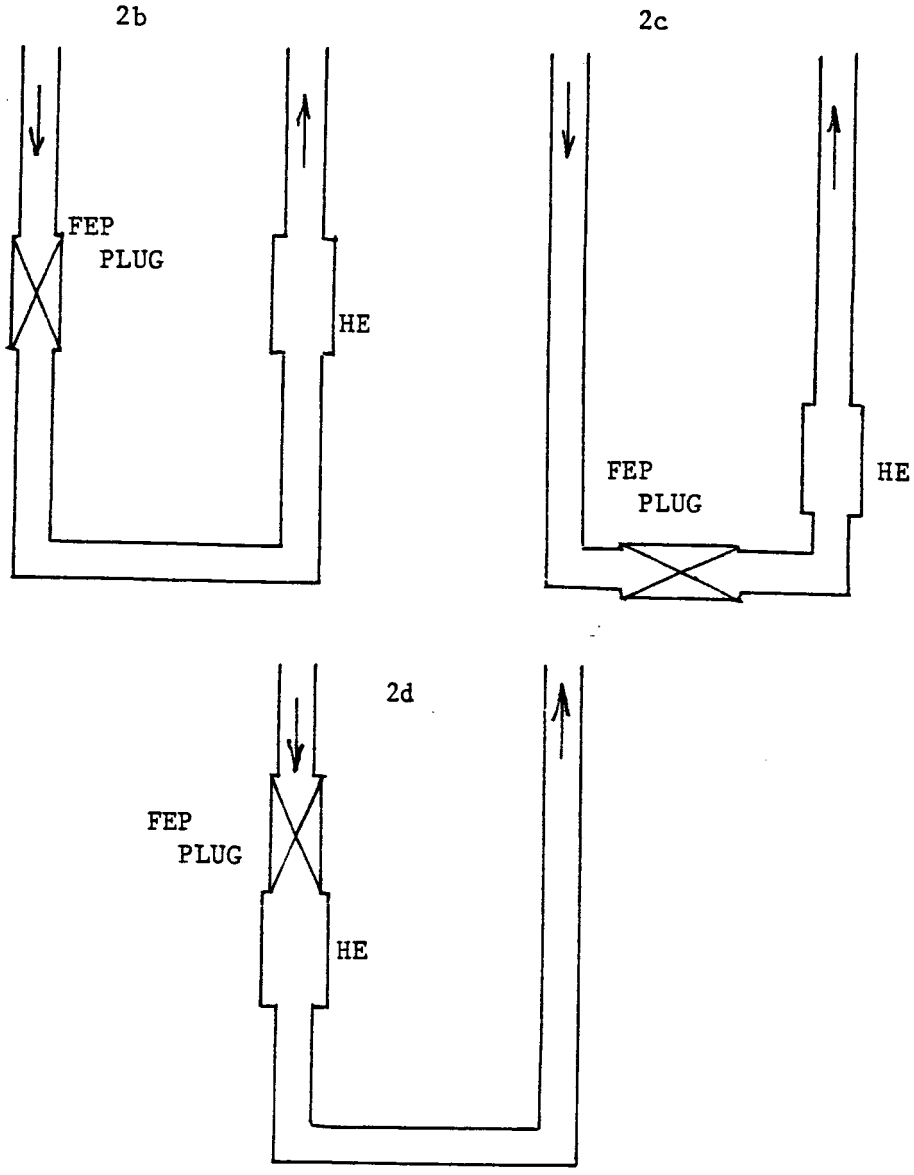

Fig. 2 (contin.)

b. FEP plug and Heater (HE) in separate legs of a U-tube assembly;
c. FEP plug at the bottom and HE in a vertical leg;
d. FEP plug and HE in the same vertical leg on the upstream side;

Vacuum can assembly , as in Fig.1 .

same vertical leg. One option is arrangement of the FEP/HE unit in the upstream leg. The other option is location in the downstream leg. The latter choice may cause a pressure decrease in the "pipe line" upstream. Consequently, in principle the liquid may reach pressures below the saturated vapor pressure curve. This danger is avoided by placing the FEP/HE unit quite close to the entrance of the "U" into the vacuum can.

The third system type is a simple transfer arrangement providing liquid movement from one open vessel into another one, e.g. concentric beakers. This transfer is accomplished via the FEP unit of the type used by S. Yuan (Ref. 3). The system is sketched in Figure 3. The liquid from an outer reservoir is transferred into the interior vessel as soon as the liquid level has fallen. No stringent time requirements have been imposed on this lab pump. Therefore, no special very fine porous medium has been used. Instead, a commercial sintered plug of relatively large filtration rating, for the limiting particle size passing through, has been utilized.

The system finally adopted is of the type shown in Figure 2d with a fine powder serving as porous medium. It is outlined in Section 4.

3. KNUDSEN EFFECTS IN POROUS PLUGS

The fine plugs needed for most FEP applications will show Knudsen effects at room temperature when light gases are passed through the plug. The mean free path becomes comparable with or exceeds the width of the local flow passage. The result is slip of the particles as they are forced through the plug by an externally applied pressure gradient. Then the flow resistance is less than the value encountered for continua, because of the reduced number of

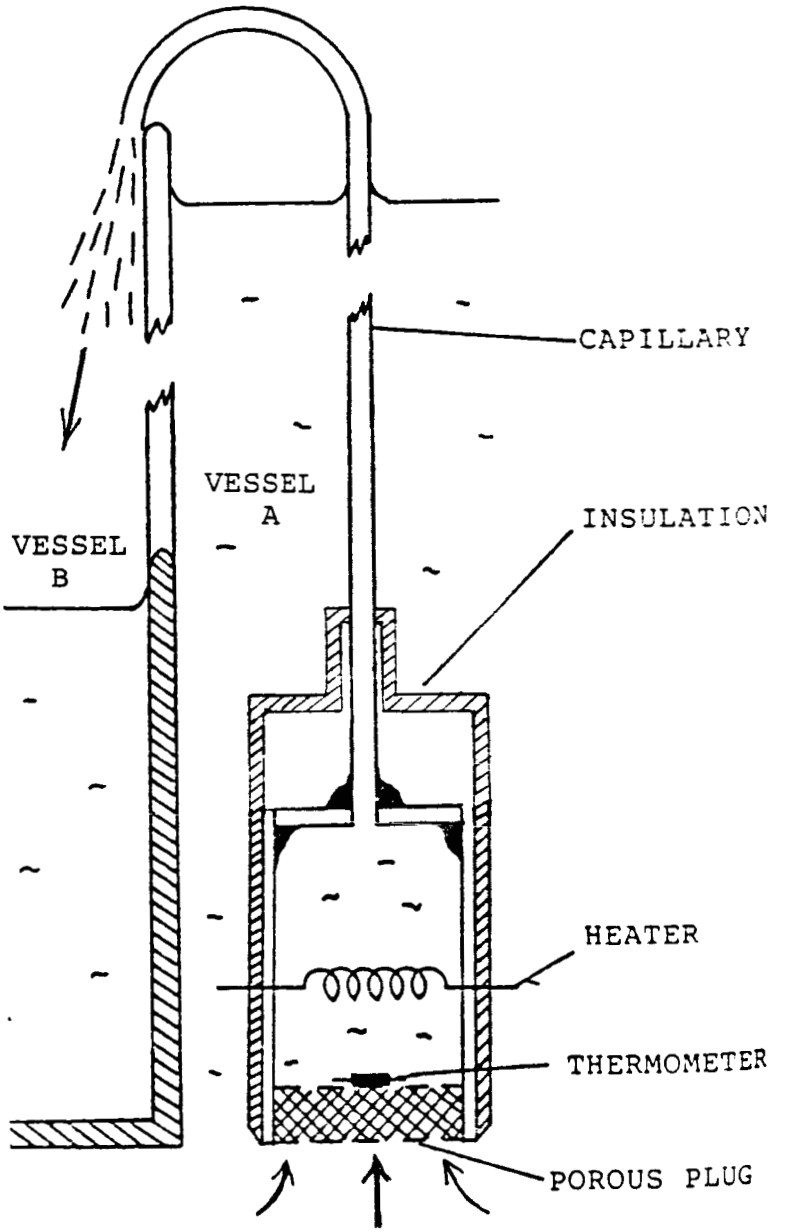

Fig. 3. Transfer system accomplishing liquid He II replenishment in vessel B using the FEP unit located in vessel A; Vessel A and B have common vapor space.
S.W.K. Yuan, Ref.3.

particle-wall collisions, compared to bulk continuum collision frequencies. The flow resistance is less than the laminar value. The latter, in the past efforts of our group, has been expressed in terms of the Darcy permeability (K_D). Therefore, any data recasting in terms of this permeability (K_D) shows up as a reduced, apparent value of K_D.

It is noted that for our measurement system, selected for rather large pores of phase separator plugs, a relatively slow flow results if previous outer plug dimensions are retained. For a reduction of measurement times, very thin plugs of rather large diameter would be needed in order to pass a large mass flow rate through the system. Further, the rotameter system used in the previous work has to be calibrated in the small mass flow rate range. These measurements initially required relatively more time than in the phase separator plug work.

Because of departures from Darcy's law, a permeability value K_p has been deduced formally assuming that a limiting value of K_D does indeed exist. The defining equation for K_p is written as mass flow rate ($\dot{m}$), divided by the fluid density ρ and the total cross section A.

$$(\dot{m}/\rho)/A = K_p(\text{grad } P)/\eta \tag{1}$$

(η = shear viscosity of the fluid, P pressure). In contrast, the Darcy permeability is defined only for continuum conditions as

$$K_D = \lim_{|\Delta P| \to 0} \{\eta(\dot{m}/\rho)/(A|\text{grad } P|)\} \tag{2}$$

Figure 4 presents an argon gas data set for room temperature and a plug with an intermediate pore size given by the manufacturer as filtration rating of 2

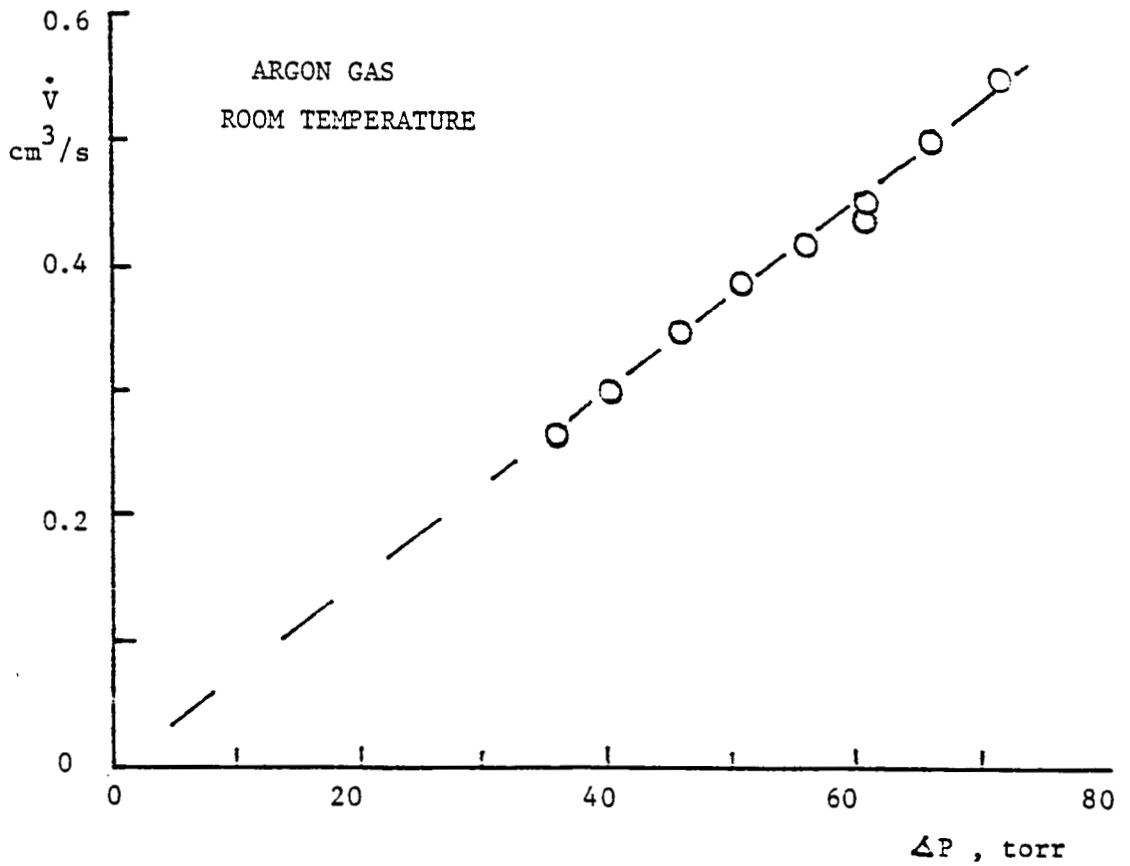

Figure 4. Porous plug data at atmospheric pressure;
Plug permeability(3.07 ± 0.01) x 10^{-10} cm^2 ;

μm; (outer diameter of the plug 1.6 cm, plug thickness 0.56 cm).

Figure 5 presents an example of experimental data obtained over a temperature range from 100 K to room temperature. These results indicate an increase in K_p as the temperature increases. As the pressure has been kept constant, the data imply a lowering of the density with temperature. As the gas becomes less dense, the particle-wall collision frequency is lowered at the same time. It is seen that the slip indicated is relatively large, i.e. Knudsen transport starts to become dominant as T is raised even more. The data indicate that near 100 K and below, the Knudsen effect is small (within the scatter of this run).

If the particular type of porous medium selected would have the same type of slip effect one would expect that there exists a universal function of the ratio (K_p/K_D) versus the appropriate length ratio. At this time, the data collected do not yet permit a verification of this similarity postulate.

4. FEP SYSTEM AND PROOF-OF-PRINCIPLE TESTS

The FEP system configuration (Fig. 2c) of Section (a) has a low dissipation rate associated with pump operation when the diameter of the FEP unit is small. The temperature difference, for instance from 1.8 K to the lambda temperature is only about 300 mK. Therefore, no drastic energy savings, and the liquid boil-off reduction associated with it, are achieved by the T-variation. The reduction in the size of the porous media particles helps in bringing about a sizable static pressure difference over an extended pressure range.

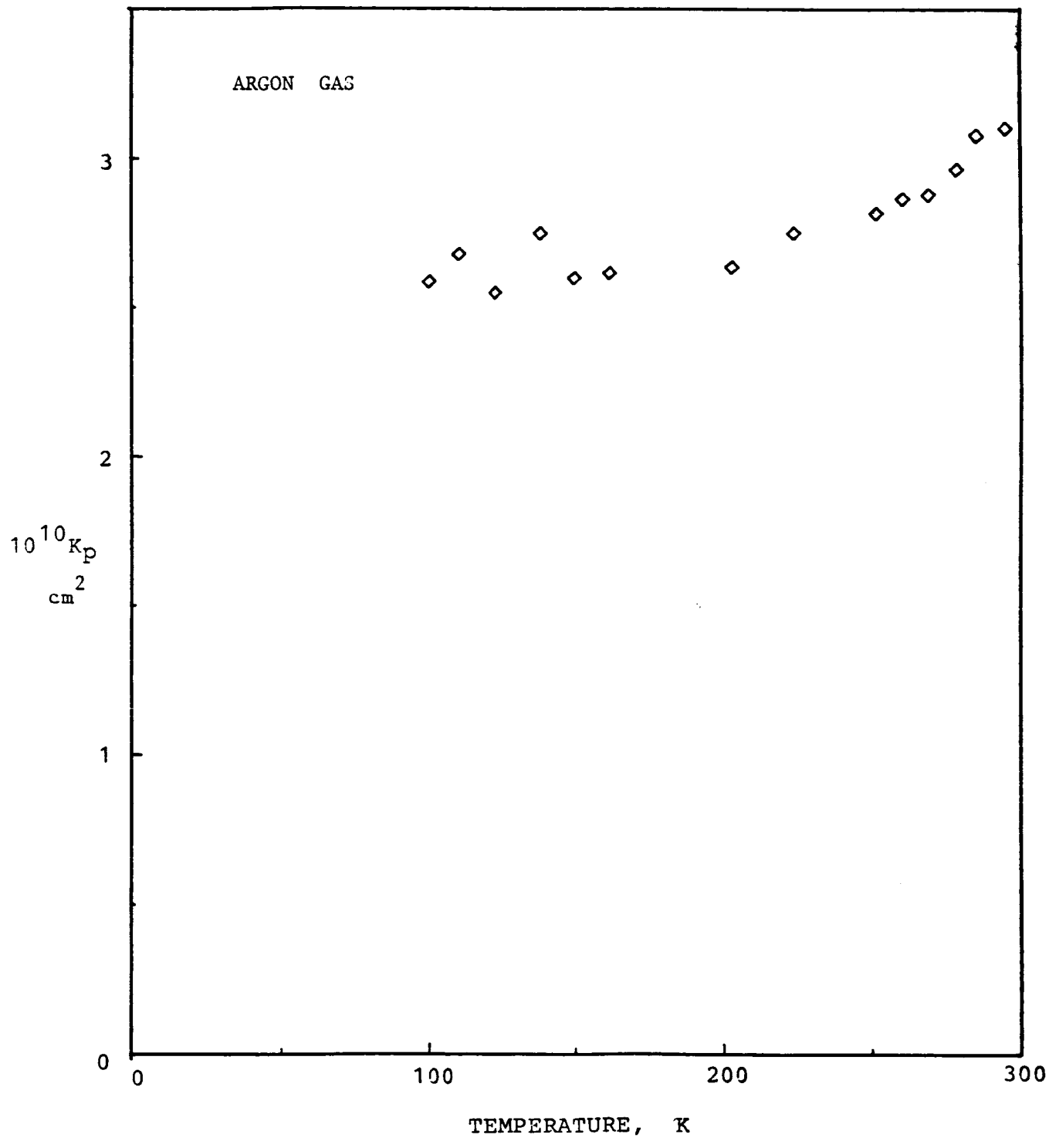

Fig. 5 . Knudsen effects seen as departures of K_p from the Darcy permeability (K_D): The slip effect increases K_p with respect to the continuum value K_D .

The tube chosen for the FEP has been a stainless steel duct available commercially (type 321; nominal sizes: diam (3/32) in. O.D. = 2.38 mm, wall thickness 10 mil = 0.254 mm). Several approaches to plug fabrication have been tried. First, a very narrow tube with a diameter of about 0.1 cm had been chosen for initial work. It turned out that particle manipulation, insertion procedures, and in particular compression and subsequent ram removal turned out to be quite inefficient. Therefore, the final choice has been the duct of the larger diameter given above.

The heater system has been selected with the aim of enlarging the active heat transfer area. A Cu tube (OFHC copper) was positioned downstream of the heater (O.D. 0.635 cm; I.D. 0.335 cm; length 2 cm). The heater windings have been would bifilarly around the tube leaving room for a thermometer measuring the solid temperature, affected by Kapitza resistance. For this first test an enhanced area has been incorporated in the heater system using Cu-powder. In a step-by-step procedure, ten layers have been applied in a hydraulic press to get a relatively uniform Cu-packing density (porosity 0.30).

The powder of the FEP is Degussa Aluminum oxide, type C. The powder has been compressed in a manner similar to the copper powder system. The Darcy permeability has been estimated to be on the order of 10^{-11} cm^2 on the basis of previous work, e.g. Reference 3 literature comparison.

The experiment has shown the following features: for the proof-of-principle runs, the pressure transducer system has been disconnected because of oscillations of temperature T, and pressure P, encountered. The rather short time remaining after the construction period induced the use of the fountain height as mass flow rate ($\dot{m}$) measure. From the known exit cross

section of the downstream exit of the U-assembly (Fig. 2d), the volumetric flow rate is available once the height H of the fountain has been observed. Thermometers, attached to the heater-FEP plug assembly showed an intermediate temperature on the FEP plug and an average heater temperature. From the latter, a ΔT on the order of magnitude of 100 mK was obtained. The related thermomechanical energy deposited in the liquid stream, per unit volume, is $\Delta P_T = \rho S(T)dT$. At low T, around 1.4 K, the pressure difference ΔP_T is of the order of 1 millibar. The observed height of several cm corresponds to this same order of magnitude. The resulting mass flow rate has been in the range from 0.5 to 10 mg/s.

Figure 6 presents data of a run with a bath near 1.8 K. The energy deposited per unit volume is given as Fig. 6a. The speed $\bar{v}_o$ of the FEP plug section is on the order of magnitude of 1 cm/s in this run. The mass flow rate $\dot{m}$ is displayed in Fig. 6b as ratio of $\dot{m}$ to the reference rate $\dot{m}_{REF}$.

The Reynolds number (Re) outside the FEP assembly is on the order of usual turbulent flow conditions. The superfluid and normal fluid are entrained such that a convenient measure for the assessment is a Re-definition based on the total density: $Re = \rho \bar{v} D \eta_h$. The diameter of the order 0.2 cm in conjunction with a speed from 1 to 10 cm/s results in Re of 5×10^3. The forced flow data, known in this range and above, appear to document "classical" turbulent friction factors.

The following conclusions result from the present proof-of-principle test. 1. Significant fountain effect pump components are accessible to performance evaluation in the absence of a complete and expensive instrumentation setup. 2. Essential features of FEP operation have been demonstrated in a

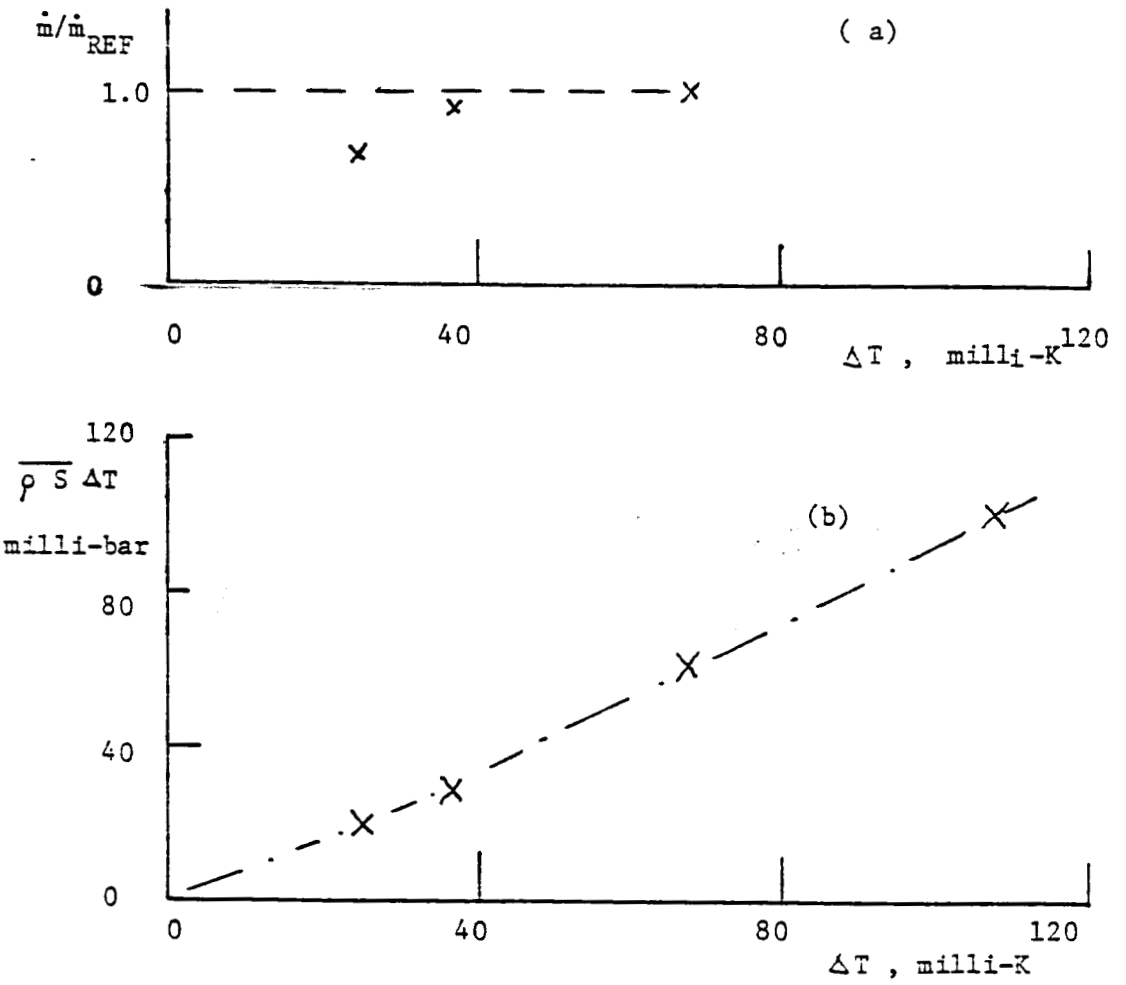

Figure 6. FEP results ;

a. Mass flow ratio versus temperature difference between FEP plug exit and bath ;

b. Energy deposited based on the temperature difference between FEP plug exit and bath ; bath temperature near 1.8 K .

simple U-tube geometry. 3. The Reynolds numbers of the resulting duct flow in the U-tube are quite comparable to a large space system in so far as turbulent flow is secured. 4. Appropriate scaling for FEP plugs ought to permit use of very small FEP plug model tests. 5. In general, scaled down versions of the entire transfer system assembly appear to be strongly suggested in order to cut costs for flight system preparations.

ACKNOWLEDGMENTS. It is a pleasure to acknowledge the dedicated assistance of F. Afifi and P. Abbassi during the experiments and data reduction. Gary Eckwortzel supported the experiments during workshop preparations, machining of parts and assembly of the FEP components. Y.S. Yi's inputs in the final documentation of the work are acknowledged with thanks. Last, not least, we are indebted to Dr. Sidney Yuan for additional information on pump operation and data for the TP-series, and for early communication of his results.

REFERENCES

1. A. Elsner and G. Klipping, Adv. Cryog. Eng. 14, 416 (1969). G. Klipping et al., Cryogenics 18, 166 (1978).

2. P. Kittel, Cryogenics 26, 59 (1986).

3. S. W. K. Yuan, Ph.D. Thesis, University of California, Los Angeles, 1985.

APPENDIX A

TRANSPORT MODE COMPARISON: FINITE THERMOMECHANICAL MASS FLOW VERSUS ZERO NET MASS FLOW

In the present Appendix, the zero net mass flow (ZNMF) mode is compared to the finite thermomechanical mass flow (FTMF). The emphasis is on similarity criteria . The two-fluid model basis for zero net mass flow is extended using the semi-empirical frame of reference of Vote et al. (Adv. Cryog. Eng. 16, 393, 1971).

Two-Fluid Model. The densities are added such that the liquid density ρ is the sum of the superfluid density ρ_s and the normal fluid density ρ_n

$$\rho = \rho_s + \rho_n \qquad (A.1)$$

Similarly the mass flux densities ($\vec{j} = \rho \vec{v}$; $\vec{v}$ velocity) are added

$$\vec{j} = \vec{j}_s + \vec{j}_n \qquad (A.2)$$

ZNMF Mode. The reader is referred to the equations presented recently at the 1985 Boston CEC (Adv. Cryog. Eng. 31, 505, 1986). The superfluid is driven, in the presence of a chemical potential gradient (grad μ), as described by the simplified equation for negligible inertia

$$\partial \vec{v}_s / \partial t + \text{grad } \mu = 0 \qquad (A.3)$$

(t time). For steady, static conditions, (A.3) yields the London pressure gradient (grad P = grad P_T) which is given by grad μ = 0; (μ chemical potential per unit mass; $d\mu = - S\, dT + dP/\rho$; S entropy per unit mass)

$$\text{grad } P = \rho S \text{ grad } T \qquad (A.4)$$

The London P-gradient is incorporated in the (truncated) equations of motion

$$\rho_n \partial \vec{v}_n / \partial t = - (\rho_n / \rho) \text{ grad } P - \rho_s S \text{ grad } T + \eta_n \nabla^2 \vec{v}_n \qquad (A.5)$$

(η_n shear viscosity of the normal fluid). The superfluid motion is phenomenologically expressed , again in a truncated form, as

$$\rho_s \partial \vec{v}_s / \partial t = - (\rho_s / \rho) \text{ grad } P + \rho_s S \text{ grad } T \qquad (A.6)$$

It is noted that the sum of Eqs. (A.5) and (A.6), for steady flow results in

$$0 = - \text{grad } P + \eta_n \nabla^2 \vec{v}_n \qquad (A.7)$$

Boundary conditions of Newtonian fluid flow are inserted to get solutions to (A.7) for the geometry under consideration. For instance the analog of Darcy convection is given by

$$\bar{v}_n = K_D \, |\text{grad } P_T| \, / \, \eta_n \qquad (A.8)$$

(K_D Darcy permeability for normal fluid flow). While (A.8) describes a class of linear , laminar flow solutions, the flow may be non-linear involving vortex shedding processes.

Heuristic arguments are employed to describe the non-linear regime. The following items are considered : Euler frame of reference, steady flow with a substantial derivative (Dv/Dt) replaced by (v grad)v terms. For instance, the sum of the normal fluid equation , (A.5) augmented by inertia terms, and the superfluid equation, (A.6) augmented by inertia, give an idea about possible relevant terms. From this approach we expect the following condition:

$$\left[(1/2) \quad \rho \, v_n^2 \, (\rho_s / \rho_n)\right] \propto \left\{ - \nabla P_T \quad + \eta_n \nabla^2 \vec{v}_n \right\} \qquad (A.9)$$

This statement may be considered for a dimensional analysis. For instance, the dimensionless normal fluid flow rate (heat flow rate) is supposed to be a function of the dimensionless pressure gradient augmented by the appropriate density ratio. The flow rate of ZNMF may be written as

$$Re \quad (\rho/\rho_s) = (\rho/\rho_s) \quad L_c \, \rho \quad \bar{v}_n / \eta_n \qquad (A.10)$$

(L_c = characteristic length, e.g. for a simple geometry). The dimensionless driving force may be written as

$$N_{\nabla P_T} \, (\rho_s / \rho_n) = (\rho_s / \rho_n) \, |\text{grad } P_T| \, \rho \quad L_c^3 \, / \, \eta_n^2 \qquad (A.11)$$

Indeed, Soloski has shown in his Ph.D. thesis that such a simple function is available to describe data, to first order, for simple geometries as long as the diameter is rather large :

$$Re \quad (\rho/\rho_s) = K_{GM} \, N_{\nabla P_T}^{1/3}$$

$$K_{GM} \approx 11.3 \qquad (A.12)$$

FTMF Mode. The system is characterized by two openings to permit flow. Thus the "closed box" of ZNMF is replaced by a flow-through system commonly desired as thermomechanical pump system (FEP= fountain effect pump). In order to avoid a large amount of vortex shedding, "weak links" are desired with only a limited kinetic energy. This ought to bring FEP operation close to the thermostatic London limit (Eq. A.4).

The two-fluid equation (A.2) is written, to first order, for negligible normal fluid flow rates:

$$j = j_s \ , \text{ or } \ \rho \bar{v} = \rho_s \bar{v}_s \qquad (A.13)$$

In the light of the driving force, non-dimensionalized, Eq. (A.11), we expect that the flow rate ought to depend on an "effective pressure gradient" $|\text{grad } P_T|(\rho_s/\rho_n)$. Further guidance is obtained from the equations of Vote et al. (op. cit.). These simplified power law approximations are modified in order to take into account the thermomechanical action by means of Eq. (A.11). In addition, the porous media component of the FEP is taken into account using the Darcy permeability for the characteristic length: $L_c = (K_D)^{1/2}$.

As in the approach of Vote et al. (op. cit.), the flow resistance ratio (R/R_N) is considered. The flow resistance is defined as

$$R = |\text{grad } P_T| \ / \ \bar{v} \qquad (A.14)$$

The reference value of R is the "normal resistance" R_N defined by Darcy's law, $\bar{v}_n = K_D \ |\text{grad } P_T| \ / \ \eta_n$, i.e.

$$R_N = (\ |\text{grad } P_T| \ / \ v \ ) = \eta_n \ / \ K_D \qquad (A.15)$$

An example of the power law approximations is the following equation of Vote et al. (op. cit.); (ζ_4 = const)

$$v = v_s \ (\rho_s/\rho) = \zeta_4 \ (\rho_s/\rho) \ |\text{grad } P_T|^{1/4} \ \eta_n^{1/2} \ \rho^{-3/4} \ L_c^{-1/4} \qquad (A.16)$$

After rearanging, the functional relationship between R/R_N and the dimensionless driving gradient may be expressed as

$$(R/R_N)(\rho_s/\rho) \ (\rho_s/\rho_n) = \phi \ (\ N_{\text{grad } P_T}^* \ ) \qquad (A.17)$$

The argument on the right hand side may be regarded as an " effective " dimensionless driving force containing the effective pressure gradient $|\text{grad } P_T^*| = |\text{grad } P_T|(\rho_s/\rho_n)$.

Footnote: The mean speed in Darcy's law is the approach speed (= volumetric flow rate per total cross section, without [illegible]. The mean intersticial speed is to be observed also in other related statements for porous media.

A P P E N D I X B

TRANSFER PUMP TESTS (TP-1) OF A SMALL LABORATORY PUMP ACTING AS THERMOMECHANICAL PUMP (FOUNTAIN EFFECT PUMP = FEP)

In the phase separator research of Sidney Yuan (Ph.D. thesis Univ. Calif. Los Angeles 1985), a pump system has been utilized to transfer routinely liquid He II from one reservoir to another reservoir. Two pumps have been built (TP-1 and TP-2). The performance of the second system has not been satisfactory. Therefore only the pump TP-1 has been employed in that work. After termination of the phase separator work (op. cit.), the upper portion of TP-1 has been removed in order to test the pump performance without additional transfer line attachments. Results of these tests are presented, mostly as results typical for a very simple system. The plug used has been a stainless steel plug (Mott, nominal filtration rating 2 μm, permeability , at room temperature 3.9 x 10 cm , thickness of plug 1/8 in . = 0. cm , diameter 1 in. = 2.54 cm).

Figures B.1 to B.3 presents thermometer runs versus (normalized) heater power at different bath temperatures. The bath temperature is the upstream temperature , seen from the point of view of pump assessment with an Euler control surface passing through the upstream and downstream end of the pump body. The upstream temperature has been kept constant . The downstream temperature is a monotonically increasing function of the heater power. The temperature difference is a non-linear function of heater power.

Figure B.1 is for a bath temperature near 1.68 K. Figure B.2 has a bath temperature of about 1.81 K. Finally, Figure B.3 has a bath temperature near 1.89 K. It is noted that the temperature difference resulting from the operation depends on the pore size of the porous medium and on the external boundary conditions, such as axial and radial heat leaks.

Figure B.4 is a plot of the heat rejected to the "environment" at low T . The total heat rejected is the sum of the heater power applied externally on the downstream side of the pump, and of the heat to be rejected upstream when temperatures are kept constant. For the latter purpose the manostat system of the present cryostat has been used noting that for high heat inputs manual control has been necessary.

Figure B.5 is a plot of representative results of the pump characteristics as resistance ratio versus dimensionless driving force. For details we refer to Appendix A. Various order parameter-dependent functions, e.g. $f(\rho_s/\rho)$, have to be incorporated to see the departures from the pump Equation (A. 16). Each point represents a set of runs. It is seen that the present pump (TP-1 modified) is described reasonably well by the power law approximation of App. A for the resistance versus driving force.

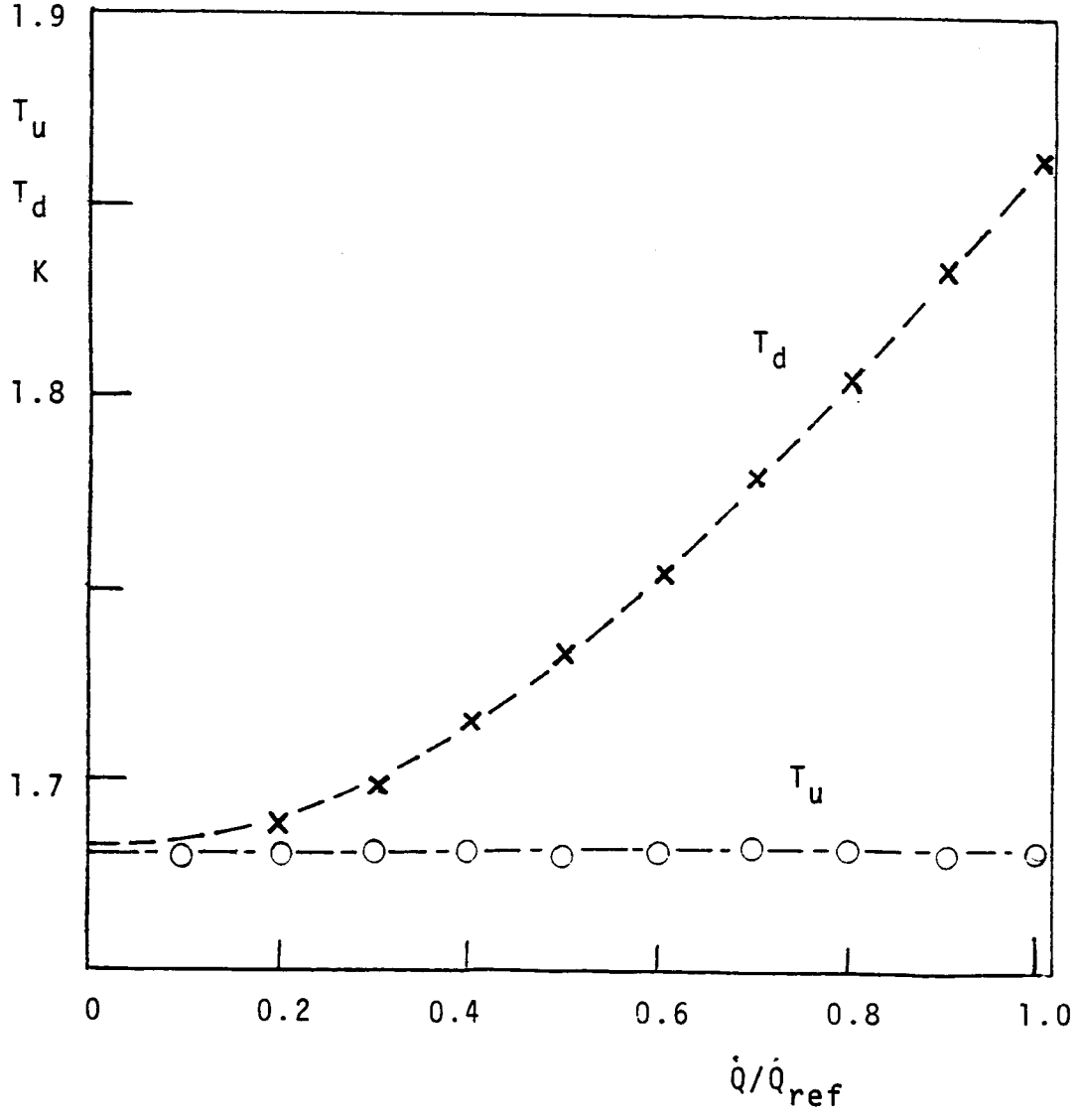

Fig.B.1.Temperatures versus heat input (normalized);
Pump : TP-1 ; T_u upstream temperature ; T_d downstream temperature .

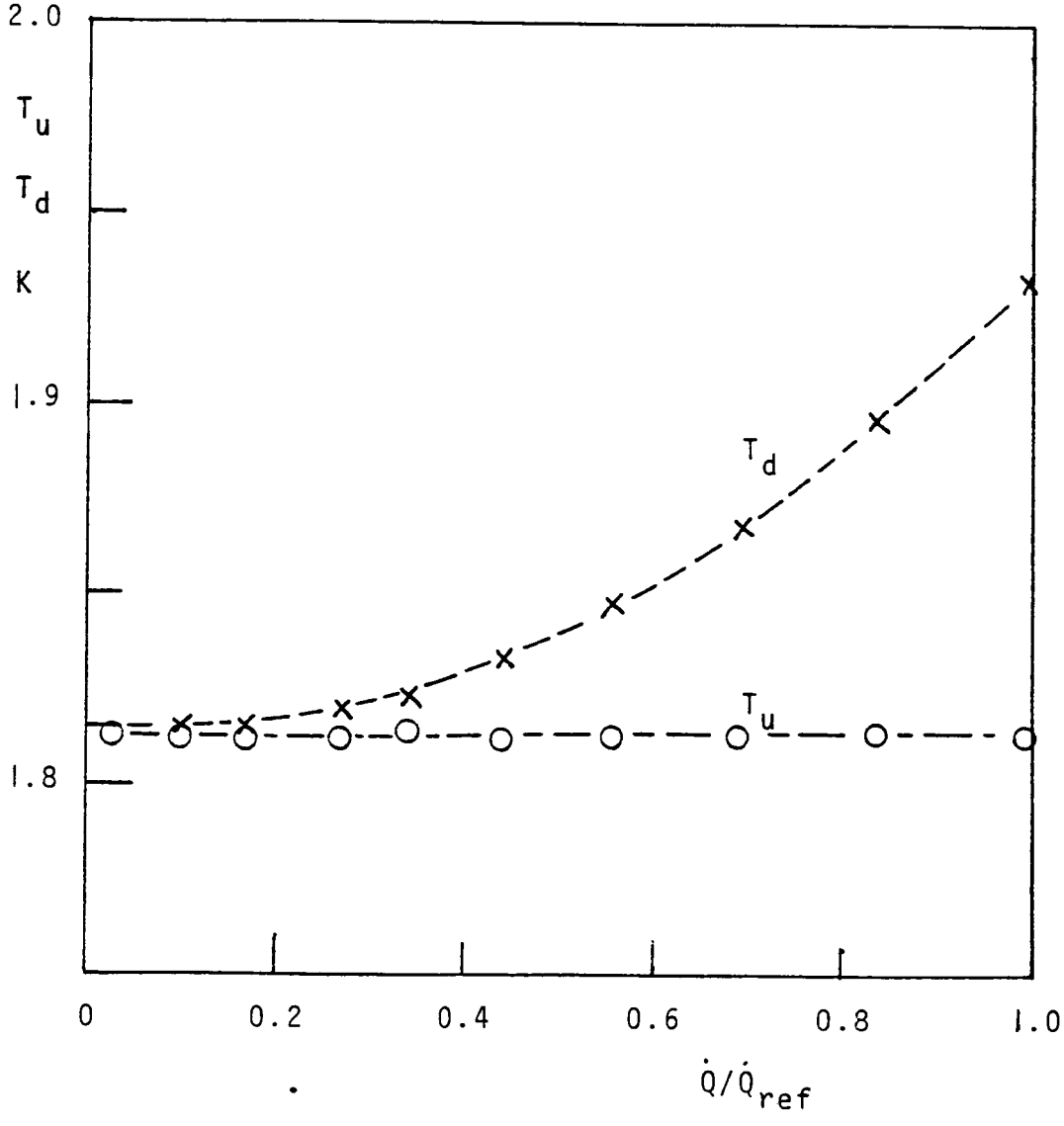

Fig.B.2.Temperatures vs. heat input (normalized); Pump : TP-1 ; T_u upstream temperature ; T_d downstream temperature .

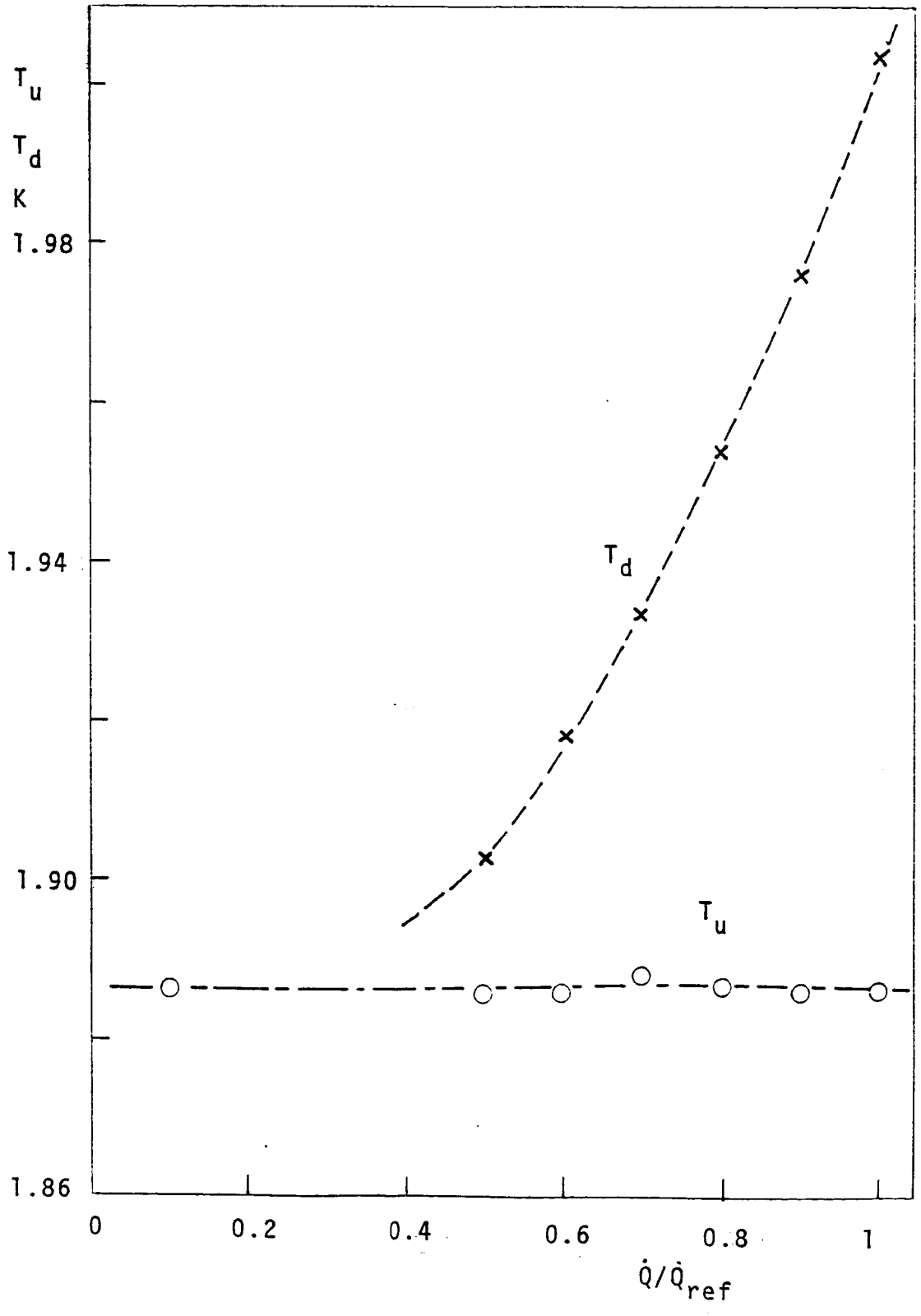

Fig. B.3. Temperatures vs. heat input (normalized) ; Pump : TP-1 ; T_u upstream temperature; T_d downstream temperature .

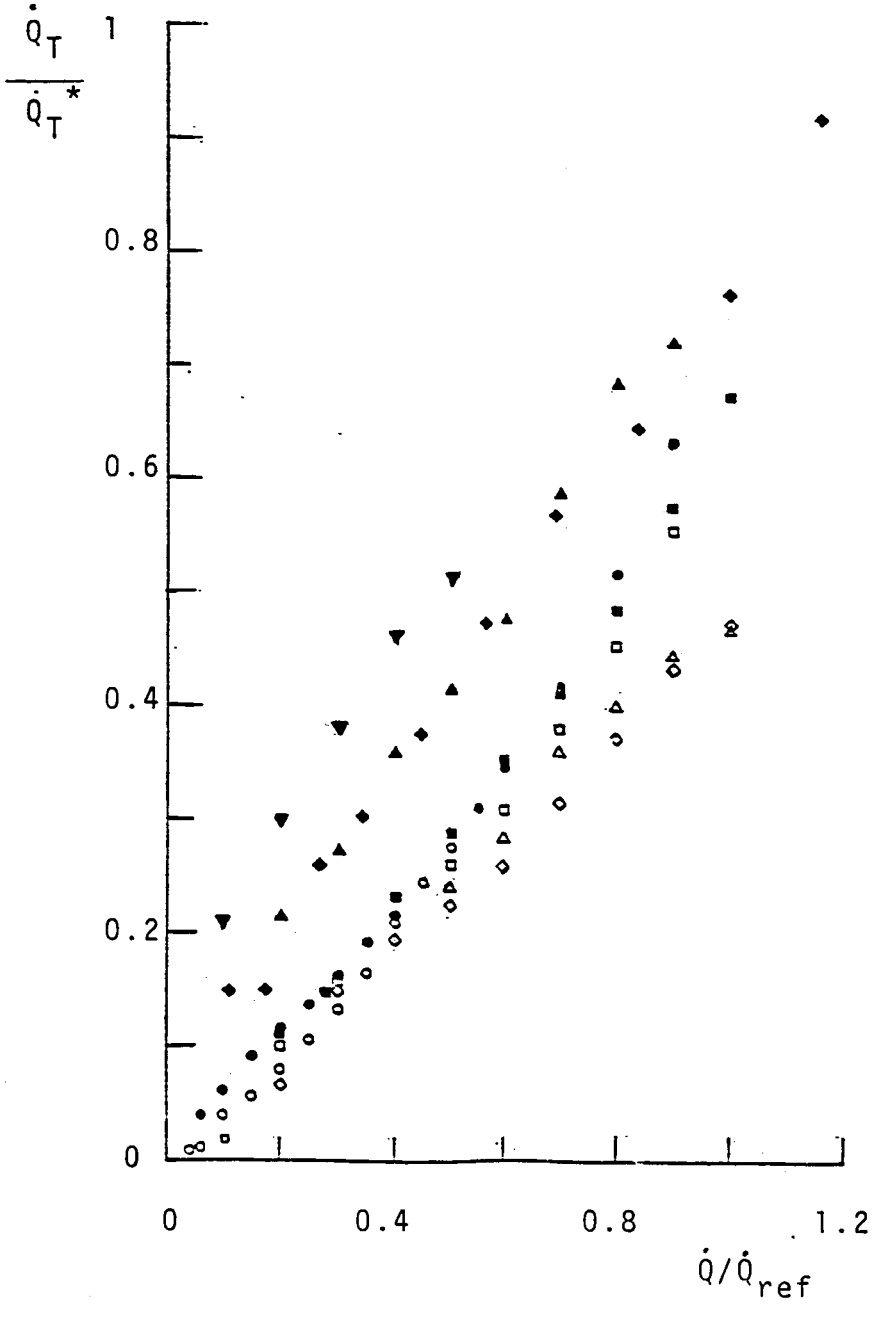

Fig. B.4. Total heat rejected, normalized as $\dot{Q}_T/\dot{Q}_T^*$, vs. heat input ratio $\dot{Q}/\dot{Q}_{ref}$.

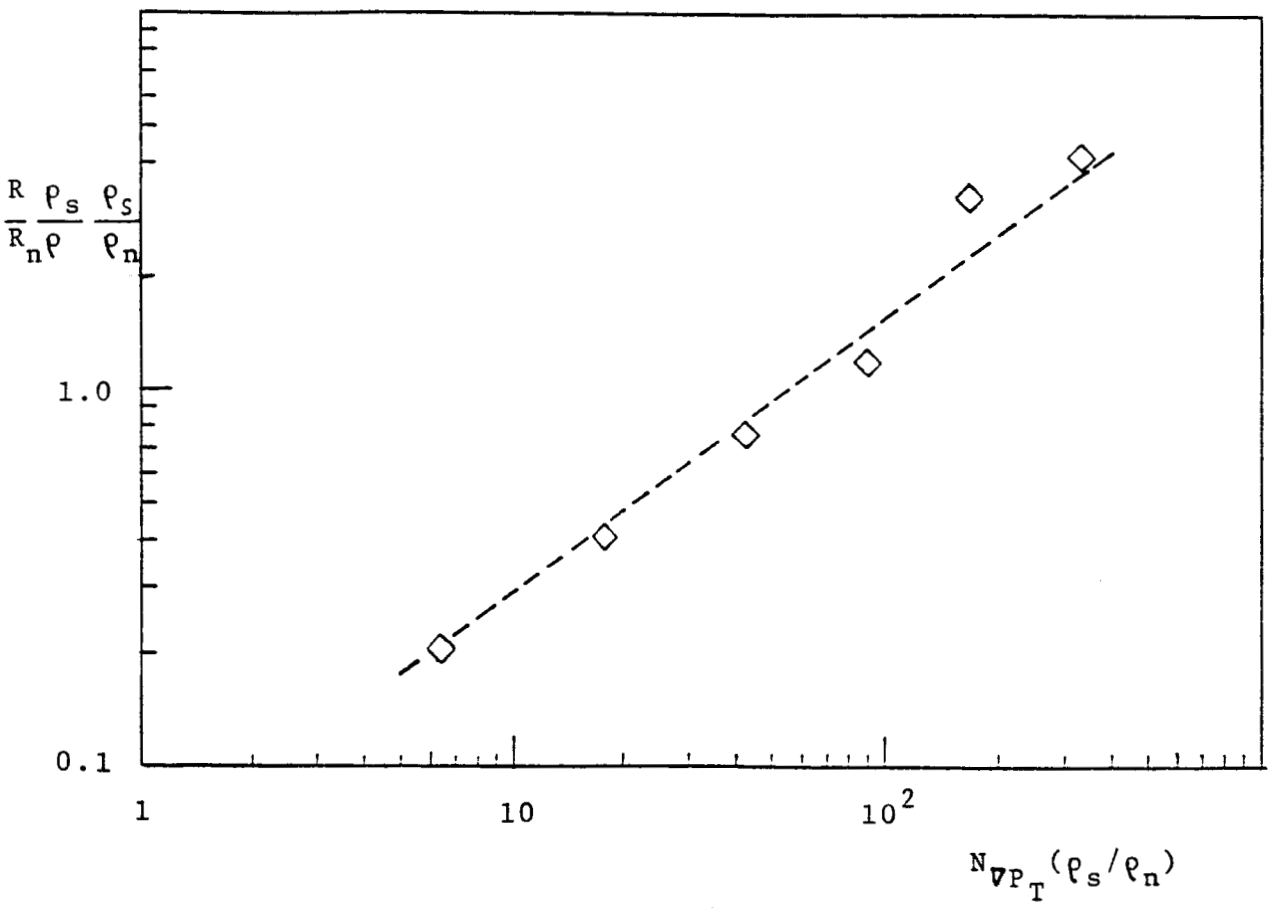

Figure B.5 Generalized resistance ratio vs. generalized driving force ($K_D = 3.4 \times 10^{-9}$ cm^2)

A P P E N D I X C

THROUGHPUT-RELATED QUANTITIES INCLUDING

KNUDSEN EFFECTS (MEAN FREE PATHS INFLUENCE)

This Appendix C outlines various items relating to fluid flow rates with emphasis on gas flow. In particular Helium-4 gas has been of great interest in the room temperature characterization of porous media, e.g. by means of the Darcy permeability. The use of Helium-4 is very compatible with the final liquid runs in so far as no elaborate purging procedures for gas exchange are needed after the room temperature runs. However, the very light Helium-4 particles are readily causing mean free path effects when the pore size is reduced below the order of magnitude of 1 μm.

Only a few literature references are mentioned : One "classical" paper is the contribution of M. Knudsen , Annalen der Physik, vol.28, pp. 75-130, 1909. Another paper dealing with He II-related properties in porous media, such as sound propagation and order parameter, is the article of M. Kriss and I. Rudnick, "Size Effect in He II as Measured by Fourth Sound, J. Low Temp. Phys. Vol. 3, pp. 339-357, 1970.

The following items are considered : Isothermal ideal gas flow at low speed (laminar flow) with pressure-independent shear viscosity (η); Knudsen's equation for circular cylinders when the slip due to long mean free paths (Knudsen effect) cannot be ignored; Mass flow meter information required for the use of rota-meters during permeability measurements.

<u>Isothermal Ideal Gas Flow</u>. Consider steady flow of gas through a duct of circular cross section $A_c = (\pi/4)D^2 = \pi R^2$; R radius = D/2 . The mass flow rate is $\dot{m} = \rho A_c \bar{v}$;

Mean speed $|\bar{v}| = \left|-(R^2/8)|\nabla P|/\eta\right|$.

Ideal gas :

$$\rho = P/(R\,T)$$

The mass flux density $\bar{j} = \rho \bar{v}$ is constant assuming a constant cross section. Thus , we have

$$\int_0^L j\,dz = -\int (R^2/8)\,P\,dP\,/(\eta\,RT) \qquad (C\text{-}1)$$

Equation (C-1) is integrated over a duct length of L . The resulting $\dot{m}$-value is proportional to $(P_1^2 - P_2^2)$. Noting that the difference in P^2 may be written in terms of the mean value of P and the difference $(P_1 - P_2)$, we have

$$j\,L = (R^2/8)\,(P_1 - P_2)\,\bar{P}\,/\,(\eta\,R\,T) \qquad (C\text{-}2)$$

The volumetric throughput $\dot{V} = \dot{m}/\rho$ is considered in molecular flow. Further, Knudsen prefers the product of $\dot{V}$ and P which he designates as Q_t . The result (C-2) may be written as

$$Q_t = \dot{m} RT = a P (P_1 - P_2)$$
$$\text{with } a = (\pi R^4 / L) / (8 \eta) \quad (C-3)$$

KNUDSEN EFFECT EQUATION. On the basis of his molecular kinetics calculations, Knudsen (op. cit) found the following result for cylinders of constant cross section: For mean free paths of gases comparable to the tube radius, a complicated law applies which extends from the Poiseuille equation for small mean free paths to the molecular flow regime. Starting from molecular flow, cylinders of circular cross section , upon an increase in the pressure P and concomitant decrease in the mean free path (MFP), the gas throughput, for a specified pressure drop, decreases toward a minimum. The minimum in Q_t will be reached when the MFP is 5 times larger than the tube radius R. At the molecular flow limit, the gas throughput Q_t is 5 % larger than the minimum. Upon a further increase in P , the throughput will rise again reaching the Poiseulle flow regime asymptotically. The Knudsen result is written as

$$Q_t = (a P + b (1 + c_1 P)/(1 + c_2 P)) (P_1 - P_2)$$

with

$$b = (4/3) (2\pi / \rho_1)^{1/2} R^3 / L$$

$$c_1 = 2 (\rho_1)^{1/2} R / \eta$$

$$c_2 = 2.47 (\rho_1)^{1/2} R/\eta \quad (C-4)$$

Mass Flow Meter Data. The rotameter results are given in Figrs. C.1 to C.3 .

TABLE C-I

Measurements of Permeability** for Ar at Room Temperature (294 K)

ΔP, torr	$\dot{V}$, $cm^3 sec^{-1}$	$10^{10} K_p$, cm^2
71.3	0.55	3.114
65.7	0.50	3.080
61.0	0.45	2.990
56.1	0.42	3.010
51.1	0.39	3.120
46.0	0.35	3.081
40.3	0.30	3.065
35.8	0.26	3.071
61.35	0.46	3.080

*The atmospheric pressure was at a constant value of 752 torr

**) $\overline{K}_p = (3.07 \pm 0.01) \times 10^{-10}$ cm^2

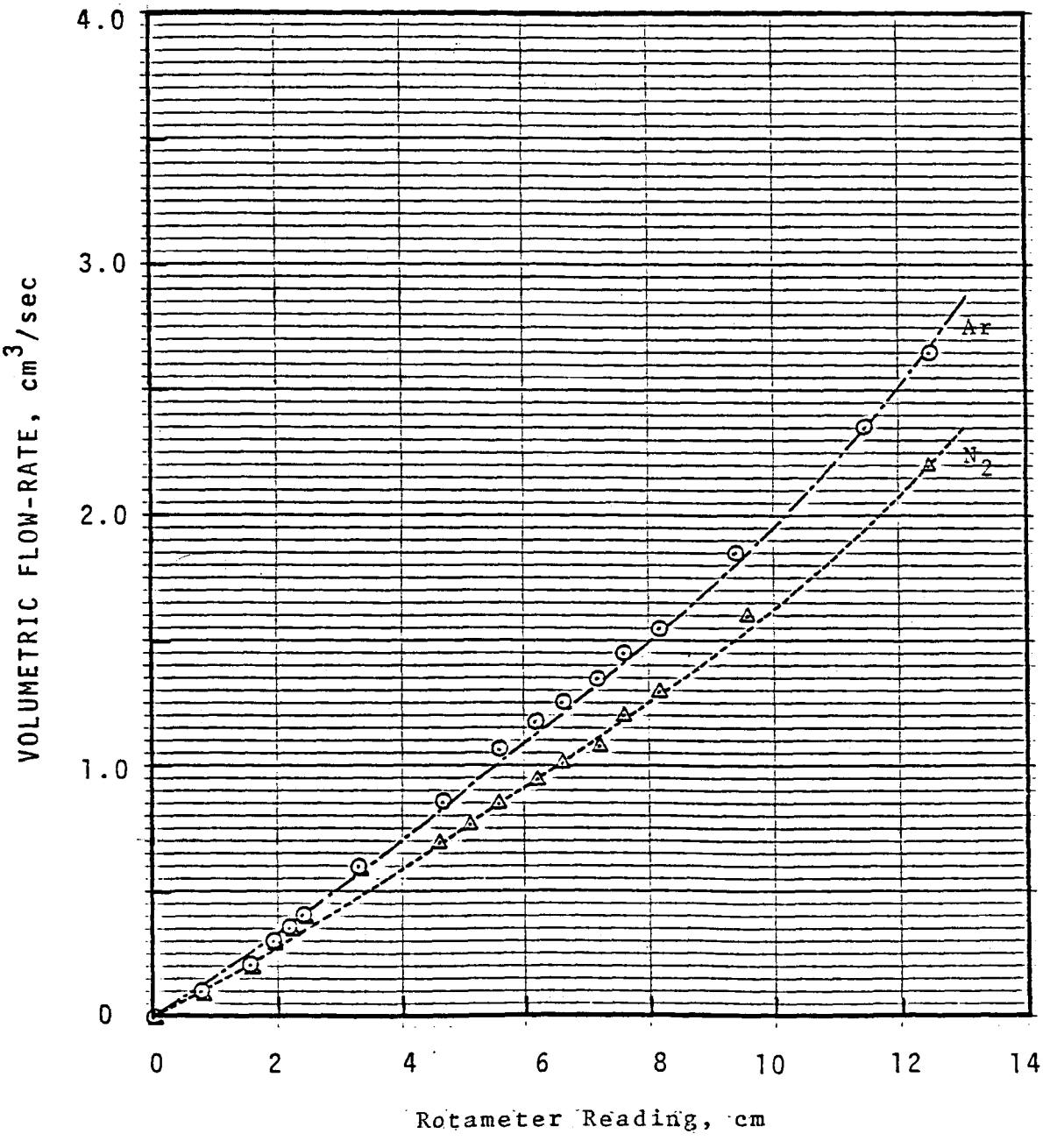

Fig. C 2. Calibration Curve for Rotameter #1
Brooks Instrument Co. Inc
Tube Size: R-2-15-AA

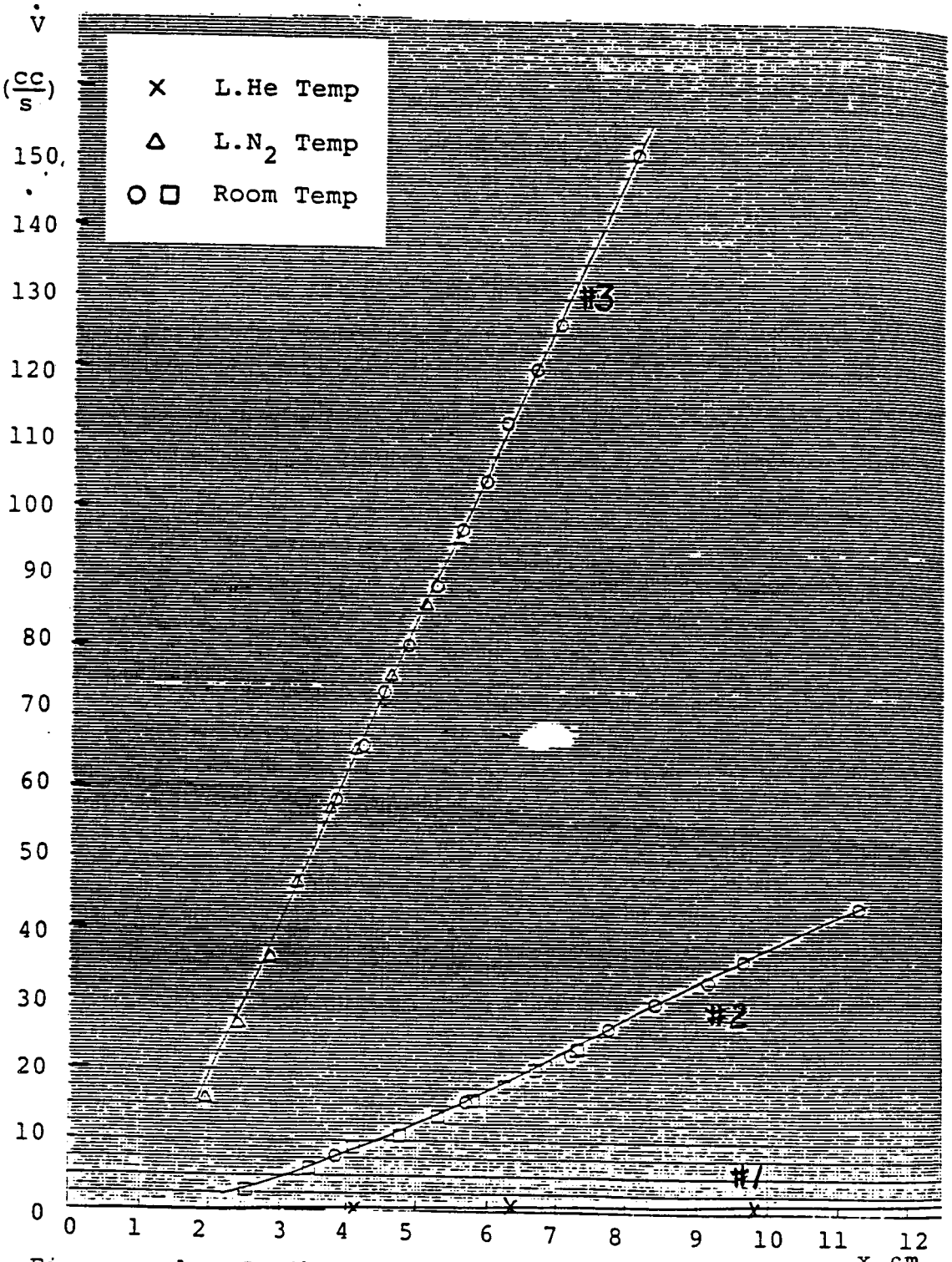

Figure C.1. Calibration curves for the rotameters.
(from Ph.D. thesis of S. Yuan)

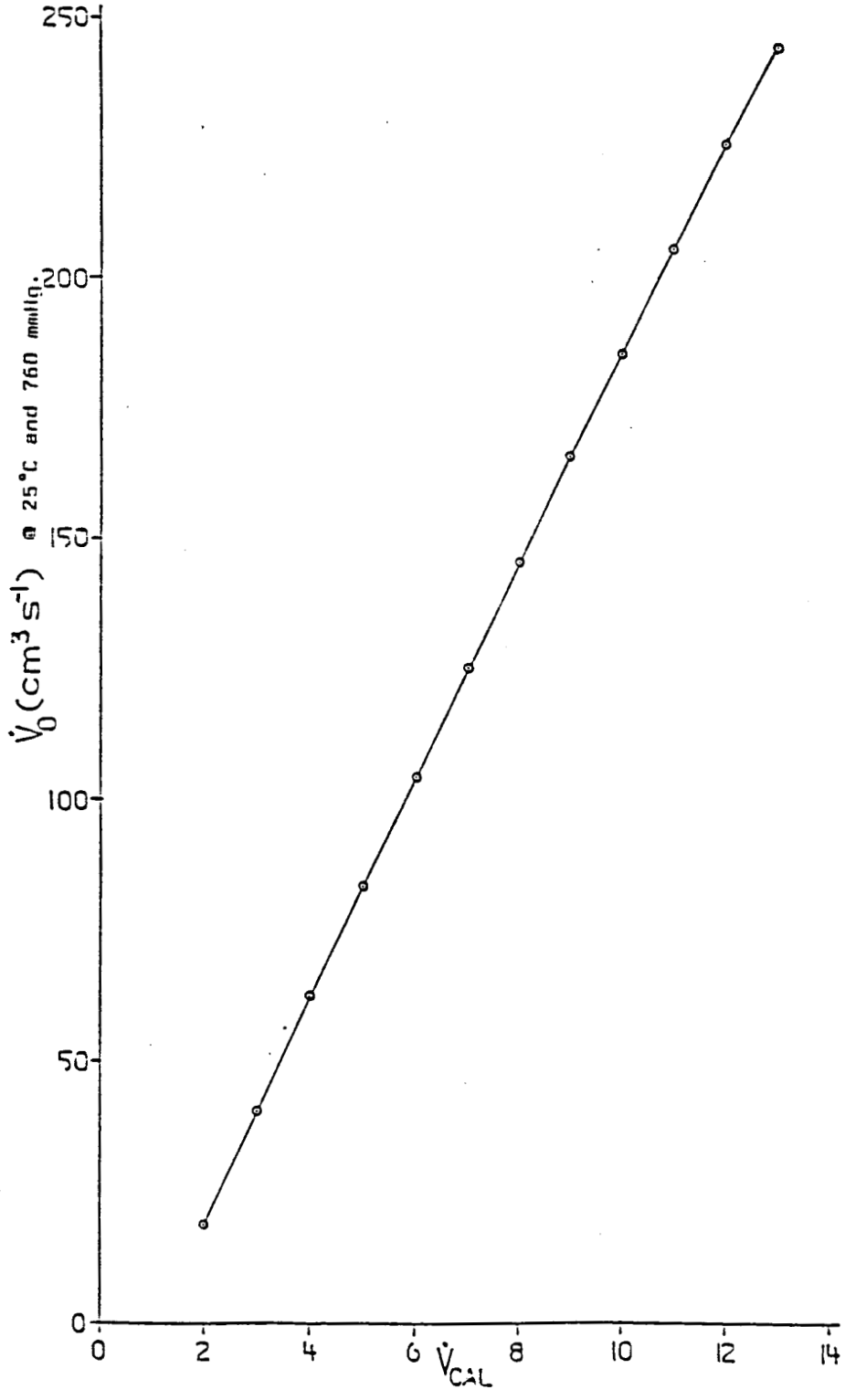

Fig. C 3. Calibration Curve for Rotameter #3
Brooks Instrument Co. Inc
Tube Size: R-2-15-C

A P P E N D I X D

PUMP PERFORMANCE PARAMETERS

The pump data obtained are assessed using the generalized resistance ratio : $(R/R_n)\ (\rho_s/\rho)\ (\rho_s/\rho_n)$. Further, the pumping rate in liters/hr is compared for pump TP-1 to the literature values.

The flow resistance , above the critical velocity, is expressed as $R = |\text{grad } P_T| / \bar{v}_n$. This resistance is related to the reference resistance of Darcy's law $R_n = \eta_n / K_D$; η_n shear viscosity, K_D Darcy permeability. At a bath temperature of about 1.8 K, the data of TP-1 are characterized by an order of magnitude of the "normal resistance" of $10^{-5} / 3 \times 10^{-9} \sim 3 \times 10^{3}$ cgs units. The flow resistance has the order of $1 \times 10^{5} / 60 \sim 2 \times 10^{3}$ cgs units. This results in a resistance ratio on the order of unity. The superfluid density ratio is about 0.7, and the super fluid to normal fluid density ratio is about 2. The dimensionless driving gradient is expressed as "effective" pressure gradient $|\text{grad } P_T|^*$, suitably normalized : $|\text{grad } P_T|^* = |\text{grad } P_T|\ (\rho_s/\rho_n)$. The dimensionless gradient is

$$|\text{grad } P_T|^*\ \rho\ L_c^3 / \eta_n^2$$

From a Darcy permeability of 10^{-9} cm one obtains the order of magnitude for the dimensionless gradient of 10 to 100 .

Table D-1 compares pump characteristics using a bath temnperature near 1.8 K and literature information. The Elsner-Klipping transfer pump has a larger cross section than the nominal area of 1 cm2 assumed. The data are available in Adv. Cryog. Engng. Vol.18, 1973, pp. 132-140.

TABLE D-1. PUMP DATA COMPARISON AT ABOUT 1.8 K

PUMP BODY	PUMP TYPE	VOLUMETRIC RATE
CERAMIC ELSNER/KLIPPING	COOLER-ACTIVATED	$\approx$ 40 LITERS/HR*
STAINLESS STEEL TP-1 (present runs)	HEATER-ACTIVATED	$\approx$ 8 LITERS/HR++

*) Nominal area of 1 cm2 inserted; $\Delta T \approx$ 0.08 K.

++) The temperature difference is about 0.2 K. It is noted that the pump without transfer tube attachment has been tested.